Antileukemic efficacy of a potent artemisinin combined with sorafenib and venetoclax

Blake S. Moses,[1,2] Samantha McCullough,[1,2] Jennifer M. Fox,[1,2] Bryan T. Mott,[3] Søren M. Bentzen,[4,5] MinJung Kim,[1,2] Jeffrey W. Tyner,[6,7] Rena G. Lapidus,[5,8] Ashkan Emadi,[5,8,9] Michelle A. Rudek,[10,11] Tami J. Kingsbury,[1,5,12] and Curt I. Civin[1,2,5,12]

[1]Center for Stem Cell Biology & Regenerative Medicine and [2]Department of Pediatrics, School of Medicine, University of Maryland, Baltimore, MD; [3]National Institutes of Health (NIH) Medical Scientist Training Program, School of Medicine, University of Alabama at Birmingham, Birmingham, AL; [4]Department of Epidemiology and Public Health and [5]Marlene and Stewart Greenebaum Comprehensive Cancer Center, School of Medicine, University of Maryland, Baltimore, MD; [6]Department of Cell, Developmental and Cancer Biology and [7]Knight Cancer Institute, Oregon Health & Science University, Portland, OR; [8]Department of Medicine and [9]Department of Pharmacology, School of Medicine, University of Maryland, Baltimore, MD; [10]Department of Medicine and [11]Sidney Kimmel Comprehensive Cancer Center, School of Medicine, Johns Hopkins University, Baltimore, MD; and [12]Department of Physiology, School of Medicine, University of Maryland, Baltimore, MD

Key Points

- Artemisinins increased CHOP, decreased MCL1, and synergized with BCL2 inhibitors and SOR against human acute leukemia cells in vitro.

- Combination of a potent artemisinin analog with SOR plus VEN reduced AML xenografts and primagrafts in vivo.

Artemisinins are active against human leukemia cell lines and have low clinical toxicity in worldwide use as antimalarials. Because multiagent combination regimens are necessary to cure fully evolved leukemias, we sought to leverage our previous finding that artemisinin analogs synergize with kinase inhibitors, including sorafenib (SOR), by identifying additional synergistic antileukemic drugs with low toxicity. Screening of a targeted antineoplastic drug library revealed that B-cell lymphoma 2 (BCL2) inhibitors synergize with artemisinins, and validation assays confirmed that the selective BCL2 inhibitor, venetoclax (VEN), synergized with artemisinin analogs to inhibit growth and induce apoptotic cell death of multiple acute leukemia cell lines in vitro. An oral 3-drug "SAV" regimen (SOR plus the potent artemisinin-derived trioxane diphenylphosphate 838 dimeric analog [ART838] plus VEN) killed leukemia cell lines and primary cells in vitro. Leukemia cells cultured in ART838 had decreased induced myeloid leukemia cell differentiation protein (MCL1) levels and increased levels of DNA damage–inducible transcript 3 (*DDIT3; GADD153*) messenger RNA and its encoded CCATT/enhancer-binding protein homologous protein (CHOP), a key component of the integrated stress response. Thus, synergy of the SAV combination may involve combined targeting of MCL1 and BCL2 via discrete, tolerable mechanisms, and cellular levels of MCL1 and *DDIT3*/CHOP may serve as biomarkers for action of artemisinins and SAV. Finally, SAV treatment was tolerable and resulted in deep responses with extended survival in 2 acute myeloid leukemia (AML) cell line xenograft models, both harboring a mixed lineage leukemia gene rearrangement and an FMS-like receptor tyrosine kinase-3 internal tandem duplication, and inhibited growth in 2 AML primagraft models.

Introduction

Most patients with acute leukemias are still treated principally with the same drug regimens used for the past 4 decades, even though these therapies result in substantial mortality and serious morbidities. Although current treatments cure most children with acute lymphoblastic leukemias (ALLs), ~20% of pediatric and ~50% of adult ALL cases still relapse, particularly in poor prognostic categories including cases harboring mixed lineage leukemia chromosomal rearrangements (MLLr).[1,2] Relapsed ALL generally requires intensive treatment, such as chimeric antigen receptor–T-cell and/or allogeneic stem cell transplantation.[3,4] Acute myeloid leukemia (AML) is cured in only ~30% of patients treated in the

---

The full-text version of this article contains a data supplement.

United States,[5,6] and standard AML chemotherapy causes severe morbidity with treatment-related deaths in ~10% of younger patients, precluding use in frail senior patients; this is a substantial limitation because the median AML patient is 67 years old.[7,8] AML is now recognized to be an extremely heterogenous disease characterized by parallel evolution and emergence in an individual patient of multiple codominant cellular clones, each harboring a different set of mutations as well as chromatin modifications that result in gene-expression abnormalities.[9,10] This molecular understanding not only rationalizes disappointing clinical observations that even mutation-targeted inhibitors have predominantly induced only partial responses as single agents in patients,[11,12] but also motivates efforts to develop novel effective, low-toxicity multiagent combinations of antileukemic agents.[13-15]

Artemisinins, a large class of derivatives of the natural compound artemisinin, are used worldwide to treat malaria with essentially no human toxicity.[16,17] Artemisinins are also active against multiple human cancer cell types,[18-29] including leukemia cells resistant to standard clinical antineoplastic drugs and harboring poor-prognosis genetic aberrations, for example, BCR-ABL, FMS-like receptor tyrosine kinase-3 internal tandem duplication (FLT3-ITD), and MLLr.[18-20,30,31] We reported that artemisinin-derived trioxane diphenylphosphate dimer 838 (ART838)[32-34] was ~88-fold more potent than artesunate (AS), the major clinical artemisinin derivative, against 23 human AML and ALL cell lines tested, with minimal in vitro toxicity to normal human hematopoietic stem-progenitor cells (HSPCs).[18] Our prior observation that artemisinins synergized in vitro with kinase inhibitors, including sorafenib (SOR), against leukemia cell lines[18] stimulated us to seek additional targeted drugs that might synergize with ART838 and SOR as a tolerable 3-drug combination. As we chose here to emphasize AMLs containing the prevalent and particularly poor-prognosis MLLr and FLT3-ITD mutations, all experiments depicted in our main figures evaluated MOLM14 and/or MV4;11 AML cell lines, each harboring both MLLr and FLT3-ITD, and additional acute leukemia cell lines and primary cases were investigated less extensively.

Leukemia cells cultured with ART838 reduced myeloid leukemia cell differentiation protein (MCL1) and upregulated integrated stress response messenger RNA (mRNA)/protein DNA damage-–inducible transcript 3 (DDIT3)/CCATT/enhancer-binding protein (C/EBP) homologous protein (CHOP), potential biomarkers for artemisinin action. SOR reduced MCL1 with minimal CHOP elevation, suggesting that SOR plus ART838 plus venetoclax (VEN; SAV) combine to target MCL1 and B-cell lymphoma 2 (BCL2) via discrete mechanisms. The SAV combination demonstrated strong synergy in vitro and clear efficacy/tolerability in AML xenograft and primagraft models. Thus, SAV warrants further development for leukemia treatment.

Methods

Antibodies, compounds, other reagents

Supplemental Table 1 details the reagents used.

Cells

Leukemia cell lines, primary cells, and luciferase (luc)-yellow fluorescent protein (YFP) labeling of AML cells are described in supplemental Table 2 and supplemental Methods. Western blots of several of the cell lines and primary cases for BCL2, MCL1, and BCLxL are in supplemental Figure 1, along with the 50% inhibitory concentrations (IC$_{50}$s) of competitive inhibitors of these BCL2-family proteins.

Cell-metabolic assays

Cell metabolism was assessed by alamarBlue assays (Life Technologies, Grand Island, NY) following the manufacturer's guidelines. Cell death was verified by Annexin V/7-aminoactinomycin D (7AAD) staining (BioLegend, San Diego, CA) per the manufacturer's guidelines.[18]

Leukemia xenograft/primagraft assays

Immunodeficient NOD.Cg-Rag1^{tm1Mom}Il2rg^{tm1Wjl}/SzJ (NRG) mice were bred at the University of Maryland Baltimore (UMB) from breeders purchased from The Jackson Laboratory (JAX; Bar Harbor, ME). Seven to 14 days after IV (tail vein) transplant of 0.5 × 10^6 to 1 × 10^6 luc/YFP-labeled leukemia cells, luminescence (AML burden) was quantitated on treatment day 0 in each NRG mouse by bioluminescence imaging (BLI) (Xenogen IVIS Spectrum; PerkinElmer, Waltham, MA). Mice were allocated to treatment groups (usually ≥5-10 mice per group) so that each group had similar average day 0 luminescence, then groups were administered drug orally (by mouth; gavage). Luminescence of each mouse was assessed over time and compared with that mouse's day 0 AML burden (fold-change). Clinical behavior, appearance, weight, and survival were also monitored.

Western blotting

Cellular protein was extracted, quantitated, electrophoresed, and western blotted with monoclonal antibodies. Antibody-specific band intensities were quantitated by densitometry (ChemiDOC XRS$^+$ and Image Laboratory system; Bio-Rad, Hercules, CA) and normalized to β-actin.[35]
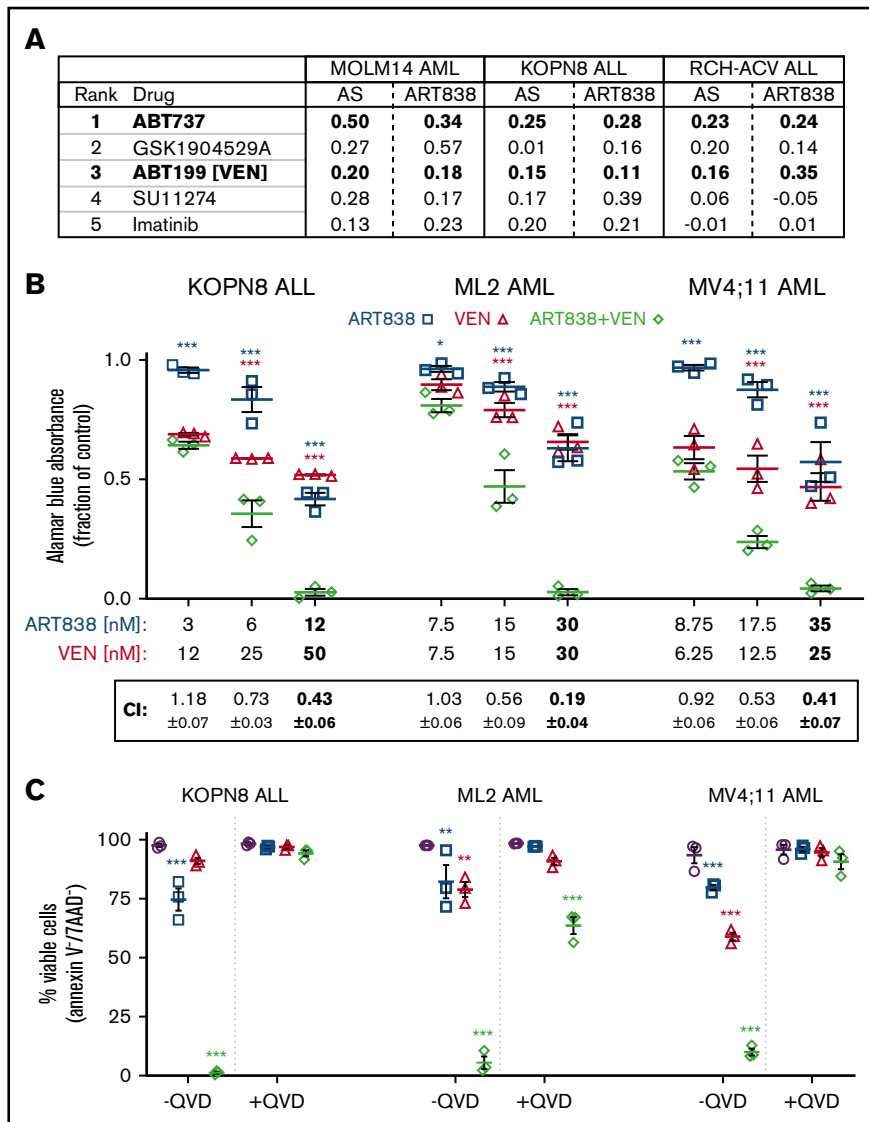
Quantitative reverse transcription PCR

Total RNA was isolated, complementary DNA was synthesized, and SYBR Green quantitative polymerase chain reaction (PCR) was performed in triplicate (Applied Biosystems QuantStudio 6 Flex and Real-Time PCR software; ThermoFisher Scientific); primer sequences are shown in supplemental Methods. Cycle threshold values were normalized to glyceraldehyde-3-phosphate dehydrogenase.[35,36]

Data analysis

The different drug treatments of cells and mice are color-coded consistently across all figures. Statistical analyses were performed using Prism 8.4 GraphPad software (San Diego, CA). Data are presented as arithmetic mean plus or minus standard error of the mean (SEM) from ≥3 independent experiments unless otherwise indicated. AML burden (luminescence) fold-change values are geometric means. To compare experimental groups, P values were calculated by analysis of variance, followed by the Dunnett multiple-comparisons test unless otherwise indicated (*P < .05; **P < .01; ***P < .001; no asterisk, P > .05). For time-to-event end points of in vivo xenograft experiments, Kaplan-Meier survival curves were compared by log-rank (Mantel-Cox).

Figure 1. ART838 synergized strongly with BCL2 inhibitors to inhibit growth and induce death of human leukemia cells. (A) Top 5 hits from the artemisinin synergy screen; BCL2 inhibitors are shown in bold. Synergy scores >0 indicate drug synergy, 0 additivity, and <0 antagonism. (B) Antileukemic synergy between ART838 and VEN against KOPN8 ALL, and ML2 and MV4;11 AML cell growth was validated by alamarBlue assays following 48-hour culture with ART838, VEN, or ART838 plus VEN.[18,52,53] Data points represent means of 3 independent experiments performed with triplicate samples plus or minus SEM, normalized to vehicle (dimethyl sulfoxide [DMSO])-treated controls set to 1. Combination indices (CIs) were determined using CompuSyn software based on Chou-Talalay principles[52,53]; CI < 1 indicates synergy; CI = 1, additivity; CI > 1, antagonism. CI at each drug's IC_{50} is shown in bold. (C) Percentage of viable cells was quantitated by flow cytometry after Annexin V/7AAD staining of KOPN8 ALL, ML2, and MV4;11 AML cells following short (18-hour) treatment with either DMSO (○; colored symbols are as shown in the key in panel A), ART838 (200 nM), VEN (50 nM), or ART838 (200 nM) plus VEN (50 nM), with and without preincubation with 10 nM pan-caspase inhibitor QVD.[54] Data points represent the percentage of viable (Annexin V⁻/7AAD⁻) cells averaged from 3 independent experiments. Statistical comparisons were performed for combination treatments vs single-drug treatments, at each drug dose (B), or for drug treatment groups vs DMSO control (C). *$P < .05$; **$P < .01$; ***$P < .001$; no asterisk if $P > .05$.

A

| Rank	Drug	MOLM14 AML		KOPN8 ALL		RCH-ACV ALL	
		AS	ART838	AS	ART838	AS	ART838
1	**ABT737**	**0.50**	**0.34**	**0.25**	**0.28**	**0.23**	**0.24**
2	GSK1904529A	0.27	0.57	0.01	0.16	0.20	0.14
3	**ABT199 [VEN]**	**0.20**	**0.18**	**0.15**	**0.11**	**0.16**	**0.35**
4	SU11274	0.28	0.17	0.17	0.39	0.06	-0.05
5	Imatinib	0.13	0.23	0.20	0.21	-0.01	0.01

Results

BCL2 inhibitors synergized with ART838 to inhibit growth and enhance apoptotic death of human acute leukemia cells

We screened a library of 111 targeted antineoplastics[37-43] to identify drugs that synergized with ART838 and/or AS.[18] To identify broad synergism against AMLs and ALLs, screening was performed in 3 human acute leukemia cell lines: MOLM14 AML (harboring MLLr KMT2A-MLLT3, FLT3-ITD), KOPN8 ALL (harboring MLLr KMT2A-MLLT1), and RCH-ACV ALL (non-MLLr) (supplemental Table 2). Each drug was ranked by "synergy score," the observed growth inhibition of the drug pair compared with the additive effect predicted by the Bliss independence model, averaged across all 3 cell lines[44-46] (supplemental Methods; Figure 1A; supplemental Figure 2A). Two of the 3 most synergistic drugs were the only BCL2-competitive inhibitors in the library: ABT737 (chemically similar to clinically tested navitoclax [NAV]; inhibits BCL2, BCLxL, and BCLW)[47,48] and

ABT199 (renamed VEN; selectively inhibits BCL2).[49] Cooperativity of ABT737, VEN, or NAV with ART838 and AS was confirmed in MOLM14 AML (supplemental Figure 2B-D). Because NAV causes clinical thrombocytopenia,[50,51] we prioritized VEN for further studies focused on MOLM14 and MV4;11 AMLs (both containing MLLr and FLT3-ITD, along with other mutations).

In Chou-Talalay drug combination index (CI) synergy analyses of 48-hour alamarBlue assays,[52,53] VEN and ART838 exhibited significant synergy at their IC_{50}s (shown in bold in Figure 1B) against KOPN8 ALL (MLLr) and 2 MLLr AML cell lines: ML2 (harboring KMT2A-MLLT4) and MV4;11, neither tested in the synergy screen (Figure 1B). Significant synergy between VEN and AS was observed against MOLM14 AML and 5 other leukemia cell lines (supplemental Figure 3).

After 18-hour culture of KOPN8 ALL, ML2, or MV4;11 AML with VEN or ART838 alone, percentages of viable (Annexin⁻/7AAD⁻) cells were only slightly reduced; these drug concentrations and relatively short culture durations were used to avoid extensive
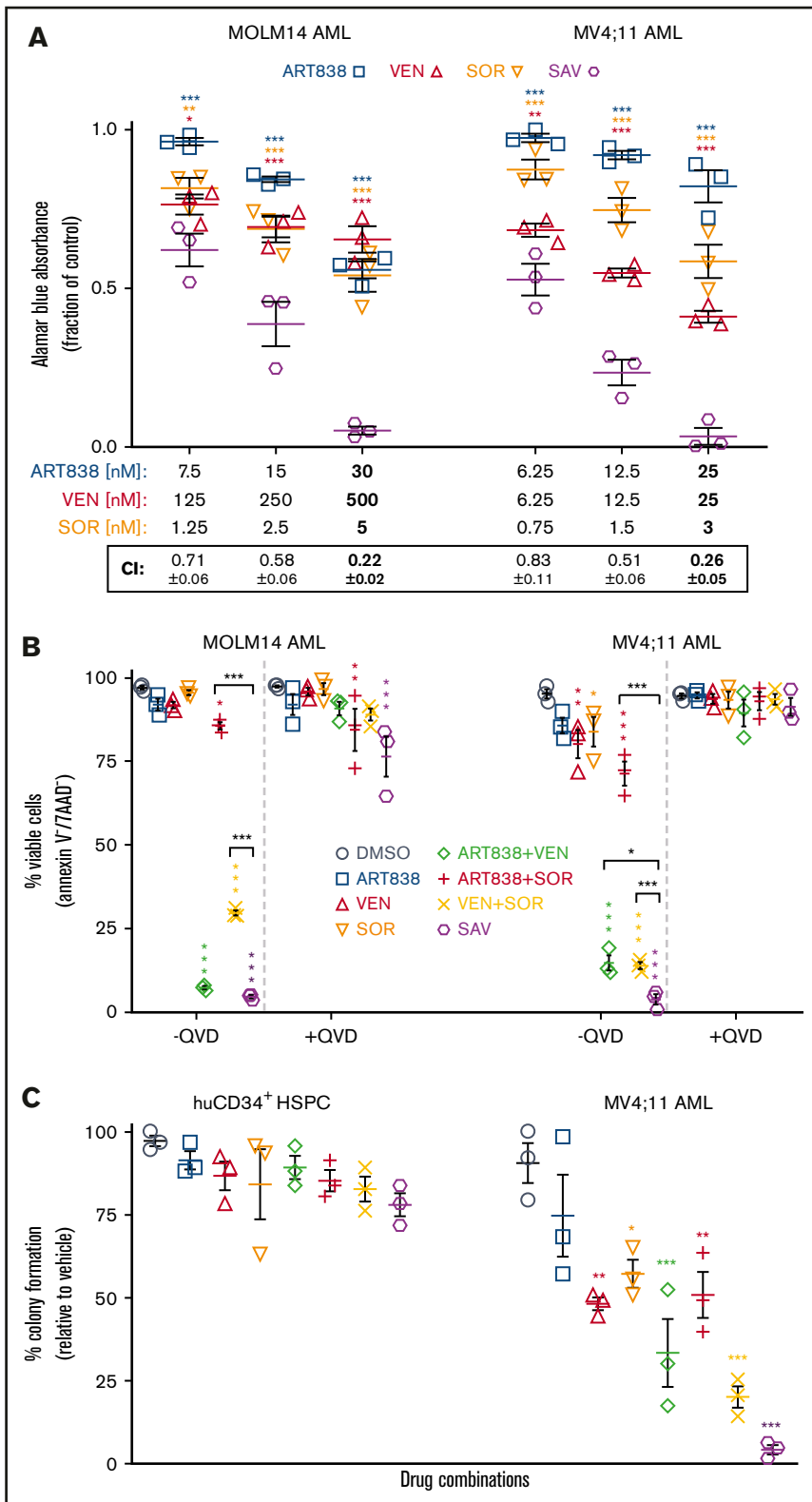
Figure 2. SOR, ART838, and VEN synergized to inhibit growth and stimulate apoptotic cell death of human AML cell lines, but spared normal human CD34+ HSPCs. (A) MOLM14 and MV4;11 AML cells were cultured for 48 hours with ART838, VEN, SOR, or SAV using 3 sets of drug concentrations by using 2 twofold dilutions from the approximate IC_{50} of each drug (in bold) for each cell line.[18,52,53] Graphs plot growth inhibition relative to DMSO, by alamarBlue assays (means of 3 experiments performed with triplicate samples plus or minus SEM). (B) Summary of 3 annexin V/7AAD flow cytometric experiments (mean plus or minus SEM) using MOLM14 and MV4;11 AML cells treated for 18 hours with DMSO, ART838 (200 nM), VEN (50 nM), SOR (5 μM), ART838 plus VEN, ART838 plus SOR, VEN plus SOR, or SAV, with or without QVD. Data points represent percentage of viable (Annexin V^-/7AAD$^-$) cells. (C) Colored symbols are as shown in the keys in panels A and B. Primary human CD34+ HSPCs, or MV4;11 AML cells were cultured with drug(s) for 24 hours, then diluted (>100-fold) and 100 to 500 cells plated in 1 mL of semisolid methylcellulose medium (H4434 for HSPCs and H4230 for MV4;11 AML cells; Stem Cell Technologies, Vancouver, Canada). Seven to 14 days later, total (erythroid plus nonerythroid for CD34+ HSPCs) colonies (≥20 cells) were enumerated.[99] Graph summarizes means of 3 independent experiments with triplicate samples plus or minus SEM. Statistical comparisons were for groups cultured with SAV vs single drugs (A) or with each drug *vs* DMSO (B-D). *$P < .05$; **$P < .01$; ***$P < .001$; no asterisk if $P > .05$.

cytolysis observed at later time points and with higher concentrations of single drugs. In contrast, parallel culture with the VEN plus ART838 combination resulted in significantly lower viable cell percentages with high levels of apoptotic/dead (Annexin$^+$7AAD$^-$ and Annexin$^+$7AAD$^+$) cells (Figure 1C; supplemental Figure 4). Apoptotic cell death was blocked by pretreatment with pan-caspase inhibitor Q-VD-OPh (QVD) (Figure 1C).[54] VEN similarly enhanced AS-induced apoptosis (supplemental Figure 5).
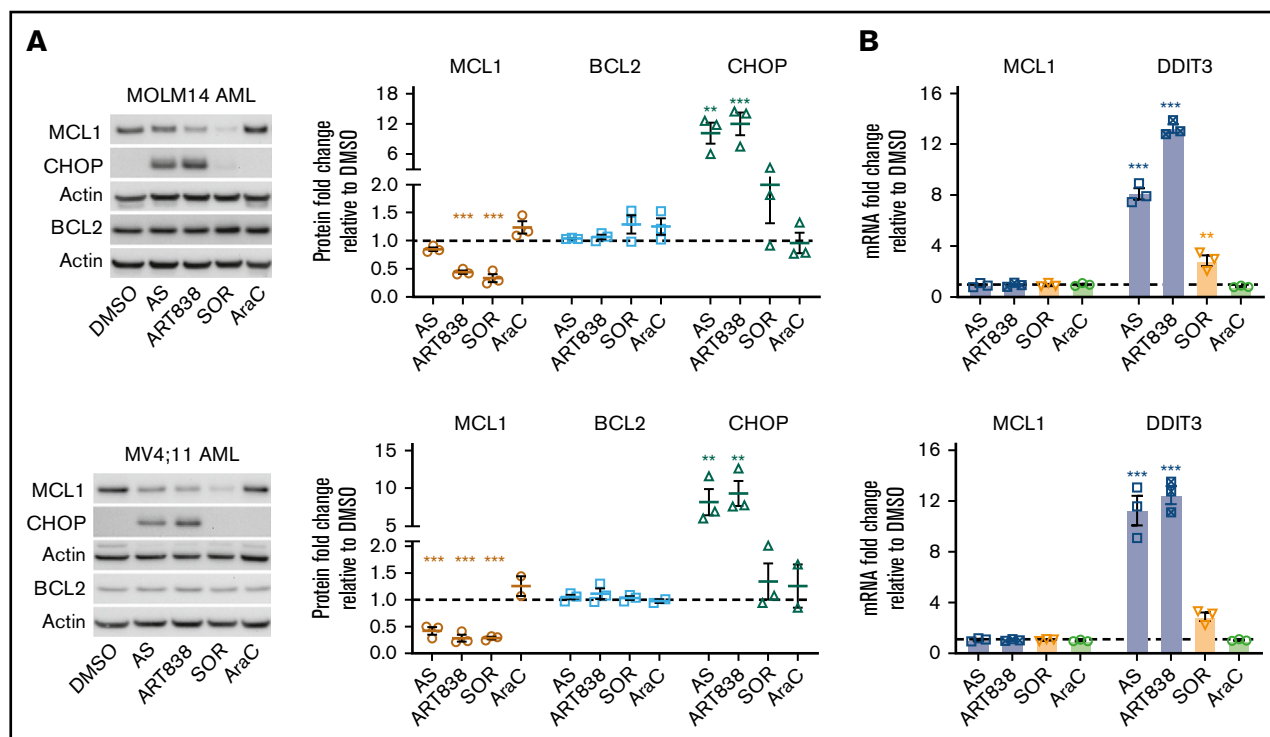
Figure 3. Artemisinins and SOR reduced MCL1 protein, and artemisinins elevated *DDIT3*/CHOP. MOLM14 and MV4;11 AML cells were incubated for 18 hours with DMSO, AS (10 μM), ART838 (200 nM), SOR (5 μM), or AraC (150 nM). (A) Western blotting was performed for MCL1 (brown circle), BCL2 (blue square), CHOP (green triangle), and housekeeping gene β-actin. Bar graphs summarize the relative fold-change of each protein level by densitometry in drug- vs DMSO-treated (represented by dotted line) cells; means of 3 independent experiments plus or minus SEM. (B) SYBR Green quantitative reverse transcription PCR was performed for *MCL1* and *DDIT3* mRNA. Cycle threshold values were normalized to housekeeping gene glyceraldehyde-3-phosphate dehydrogenase and fold-change relative to DMSO (represented by dotted line) was graphed; means of 3 independent experiments with triplicate samples plus or minus SEM. Statistical comparisons were performed for drug- vs vehicle (DMSO)-treated cells. *$P < .05$; **$P < .01$; ***$P < .001$; no asterisk if $P > .05$.

The SAV combination potently inhibited leukemia cell growth but spared normal HSPCs

Because we found previously that SOR synergized with artemisinins,[18] we next tested the antileukemic activity of the SAV combination. In 48-hour alamarBlue assays with each drug at ~25%, ~50%, and ~100% (shown in bold in Figure 2A) of its IC$_{50}$ against MOLM14 and MV4;11 AML cells, SAV demonstrated synergistic CI values (Figure 2A).[52,53] Similar results were observed testing KOPN8 ALL and ML2 AML cells (supplemental Figure 6). SAV induced ≥95% apoptosis in flow cytometric assays of the tested 3 leukemia cell lines and 6 primary AML/ALL cases. SAV was statistically superior to VEN plus SOR against MV4;11, MOLM14, AML45, and AML1526. Although SAV was not substantially superior to VEN plus SOR in all tested cell lines/primary cases, it is possible that the high efficacy of VEN plus SOR obscured the additional contribution of ART838 and/or the high spontaneous apoptosis of primary cells cultured ex vivo reduced the dynamic range of these assays (Figure 2B; supplemental Figure 7).

After culture of primary human CD34$^+$ HSPCs with SAV, normal hematopoietic colonies were reduced by only ~20% (Figure 2C) relative to vehicle, similar to the effects of the single drugs. In contrast, parallel culture of MV4;11 cells with SAV reduced total AML colonies by >95% (Figure 2C).

Artemisinins and SOR each reduced MCL1 protein levels, but by distinct mechanisms

Because artemisinins, including dihydroartemisinin (DHA), the active metabolite of several artemisinins, reduce MCL1 protein levels via the integrated stress response pathway[55] in ALLs harboring BCR-ABL,[20] we assessed whether ART838 (not metabolized to DHA[18,34]) reduced MCL1 in AML/ALL cell lines lacking BCR-ABL. To avoid nonspecific cell death–associated reduction of MCL1, we used drug concentrations and a short (18-hour) artemisinin exposure where >85% of cells remained viable (Figure 2B). AS, ART838, or SOR reduced MCL1 protein levels in MOLM14, MV4;11, ML2 AML, and KOPN8 ALL cell lines (Figure 3A; supplemental Figure 8). Specificity was observed, in that none of these drugs affected BCL2 or BCLxL protein levels, VEN increased MCL1 levels, and cytosine arabinoside (AraC; the most effective clinical drug against AML[56,57]) did not affect MCL1 levels. MCL1 mRNA levels were not changed by ART838 or AS (Figure 3B; supplemental Figure 9), and ART838 did not significantly alter MCL1 protein half-life in KOPN8 ALL or ML2 AML cells (supplemental Figure 10). Importantly, all of these leukemia cell lines are sensitive to the selective competitive MCL1 inhibitor S63845[58] (IC$_{50}$ range, 7-177 nM; supplemental Figure 1B), suggesting that reduction of MCL1 protein levels in these cells would similarly result in cell death.
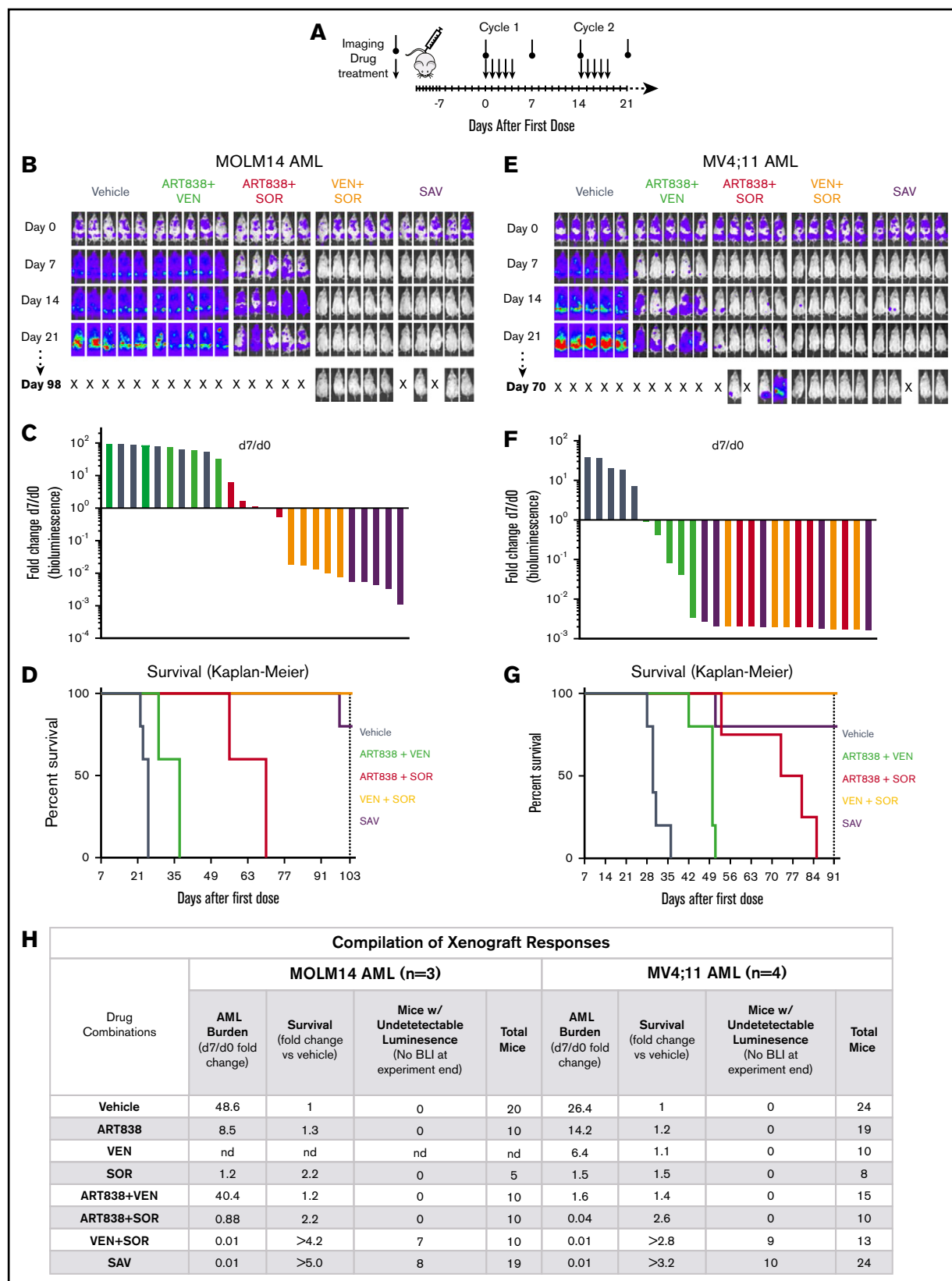
Figure 4. The VEN plus SOR and SAV combinations induced deep, long remissions in MOLM14 and MV4;11 AML xenografts. (A) Schedule for drug treatment and BLI. Drugs (50 mg/kg/d ART838, 150 mg/kg/d VEN, and/or 30 mg/kg/d SOR) were administered by mouth (via gavage) on this 5-day on/9-day off schedule for ≥5 identical 5-day treatment cycles. (B-D) NRG mice were transplanted IV with luc/YFP-labeled MOLM14 AML cells or (E-G) luc/YFP-labeled MV4;11 AML cells 10 days prior to

Culture of MOLM14 and MV4;11 AML cells with ART838 or AS, but not AraC, induced more than fivefold to 10-fold elevations in levels of the integrated stress-response protein CHOP (Figure 3A; supplemental Figure 8) and *DDIT3* mRNA (*GADD153* [encodes CHOP protein] Figure 3B). SOR caused only 1.3-fold to 3.6-fold increases in DDIT3/CHOP levels. In time-course experiments, *DDIT3* mRNA levels were elevated in MV4;11 AML cells cultured for ≥4 hours with ART838 (supplemental Figure 11A). These in vitro observations translated to in vivo, with a twofold to fourfold increase in *DDIT3* mRNA in cells harvested 6 to 8 hours after ART838 administration from heavily leukemia-infiltrated bone marrow and spleens of luc/YFP-labeled MV4;11-bearing mice (supplemental Figure 11B). In contrast, deoxyART838, which lacks endoperoxide pharmacophores,[59,60] neither reduced MCL1 levels nor elevated CHOP levels (supplemental Figure 12). Additionally, levels of several other known MCL1-regulatory proteins, including translation initiation factor eIF4B,[61] ubiquitin-associated protein FBXW7,[62] and deubiquitinase USP13,[63] were not altered by culture with any of these drugs (supplemental Figure 13A). GSK3β, another known regulator of MCL1,[64] was not altered by ART838 or AS, whereas SOR treatment reduced the phosphorylated (inactive) form of GSK3β in MOLM14 AML cells (supplemental Figure 13B), consistent with previous reports.[65] These results suggest that ART838 and SOR downregulate MCL1 protein levels mainly by distinct mechanisms.

ART838 was stable in plasma and microsomes

For in vivo preclinical and potential clinical use, we measured the stability of ART838 in human and mouse plasma and liver microsomes. Under all tested conditions, ART838 was degraded by ≤20% (supplemental Table 3).

## ART838 MTD and pharmacokinetics in NRG mice

In pilot experiments in NRG mice, we determined the single-dose maximum tolerable dose (MTD) for ART838 as 250 mg/kg by mouth and the repeated dose MTD for ART838 as 50 mg/kg daily ×5 by mouth (supplemental Methods). Plasma concentrations of ART838 were >30 nM (the in vitro IC_{50} for ART838 against MOLM14) for ~8 hours, suggesting that daily dosing is reasonable. Based on these results, we developed a tolerable 5-day on/9-day off cyclic SAV treatment dose schedule (Figure 4A).

In vivo SAV, or SOR plus VEN, treatment of MOLM14 and MV4;11 AML xenograft models resulted in deep responses and extended survivals

Novel drugs and combinations initially developed via in vitro experiments require in vivo evaluation to better model patient treatment. In several experiments, we treated NRG mice bearing luc/YFP-labeled MOLM14 or MV4;11 AML xenografts with ≥5 cycles of ART838, VEN, and/or SOR. As compared with treatment with vehicle, monotherapy with either SOR, ART838, or VEN slowed the increase in AML burden at day 7 (taken as time point of near-maximal response to the first treatment cycle). However, none of the monotherapies reduced day 7 MOLM14 or MV4;11 AML burden to levels substantially below day 0 luminescence. These results were confirmed at day 14, the earliest time when NRG mice can tolerate a second treatment cycle (supplemental Figures 15A-C and 16B-D, visualized best in the waterfall plots and line graphs). Consistent with these observations, Kaplan-Meier survival curves of MOLM14 or MV4;11 AML xenograft-bearing mice administered the 3 monotherapies were not markedly longer than for vehicle-treated mice in these experiments involving mice with substantial initial AML burdens (supplemental Figures 15 and 16).

Supplemental Figures 15A and 16A provide direct comparisons of results of the SAV regimen vs each of the 2-drug combinations against MOLM14 and MV4;11 AML xenografts, respectively; for convenience, the most relevant data are also shown in Figure 4, panels B-D and E-G. SAV treatment of MOLM14 xenografts resulted in the greatest fold reduction of day 7 AML burden, followed by VEN plus SOR, ART838 plus SOR, and ART838 plus VEN; day 7 AML burden was 83- and 250-fold reduced from day 0 by VEN plus SOR and SAV, respectively (Figure 4B-C). Assessments at subsequent time points confirmed the day 7–based rank order of AML burden reductions following SAV or the 2-drug combinations (supplemental Figure 15A). Survival was fourfold increased for both SAV and VEN plus SOR compared with vehicle (Figure 4D). All 5 mice from the VEN plus SOR group and 3 of 5 (1 mouse censored due to death with low AML burden) from the SAV group had undetectable AML burdens on day 103 (treatment ended on day 60; supplemental Figure 15A).

Figure 4. (continued) initial BLI. Based on Xenogen quantification of baseline luminescence on day 0, mice were placed into experimental groups balanced for luminescence (5 mice per group), and drug treatment initiated. (B,E) BLI of each mouse for the initial 21 days and last imaging day (day 98 in panel B, day 70 in panel E of these 2 experiments involving AML xenograft-bearing mice treated with either vehicle, 2-drug, or SAV combinations). Luminescence intensity color coding was scaled to the same minimum and maximum across all individual experiments. (C,F) Waterfall plots representing fold-change in luminescence on day 7 vs day 0 for each mouse. (D,G) Kaplan-Meier survival curves. Experiments were terminated on day 103 for MOLM14 AML and day 91 for MV4;11 AML (vertical dotted line). One SAV mouse (D) and 1 ART838 plus SOR mouse (G) died unexpectedly with low AML burden and were censored. (D) Comparisons of vehicle vs ART838 plus VEN, vehicle vs ART838 plus SOR, vehicle vs VEN plus SOR, vehicle vs SAV, SAV vs ART838 plus VEN, SAV vs ART838 plus plus SOR all have *P* < .005. (G) Comparisons of vehicle vs ART838 plus VEN, vehicle vs ART838 plus SOR, vehicle vs VEN plus SOR, vehicle vs SAV, SAV vs ART838 plus VEN have *P* ≤ .005; SAV vs ART838 plus SOR all have *P* < .05. *P* values were calculated by log-rank (Mantel-Cox) test. (H) 3 similar MOLM14 AML and 4 similar MV4;11 AML xenograft treatment experiments were performed, and results summarized. Treatment response outcomes were: Leukemia response quantitation via fold change in AML burden (luminescence) on day 7 *vs* day 0 for each mouse (geometric means for each treatment group were averaged across all experiments); survival (fold change in median survival vs vehicle; fold changes were averaged for each treatment group across all experiments). In the survival columns, > indicates that groups contained mice with no detectable luminescence (above background, 5.7×10^5 photons per mouse based on intensity values from nonleukemia-bearing mice) on the last BLI done in the experiment. In the aggregated results of all experiments using the MOLM14 AML model, 7 mice (70%) had no detectable luminescence (above background) after treatment with VEN plus SOR and 8 mice (42%) with SAV (at 42-101 days after treatment completion). In the aggregated results of all experiments using the MV4;11 AML model, 9 mice (69%) had no detectable luminescence (above background) after treatment with VEN plus SOR and 10 mice (42%) with SAV (at 9-45 days after treatment completion). Inverse association between the fold-change (day 7/d 0) in AML burden and the fold-change in median survival relative to vehicle for MOLM14 or MV4;11 AML were calculated using the Spearman rank correlation coefficient. nd, not done; "X", mouse death.
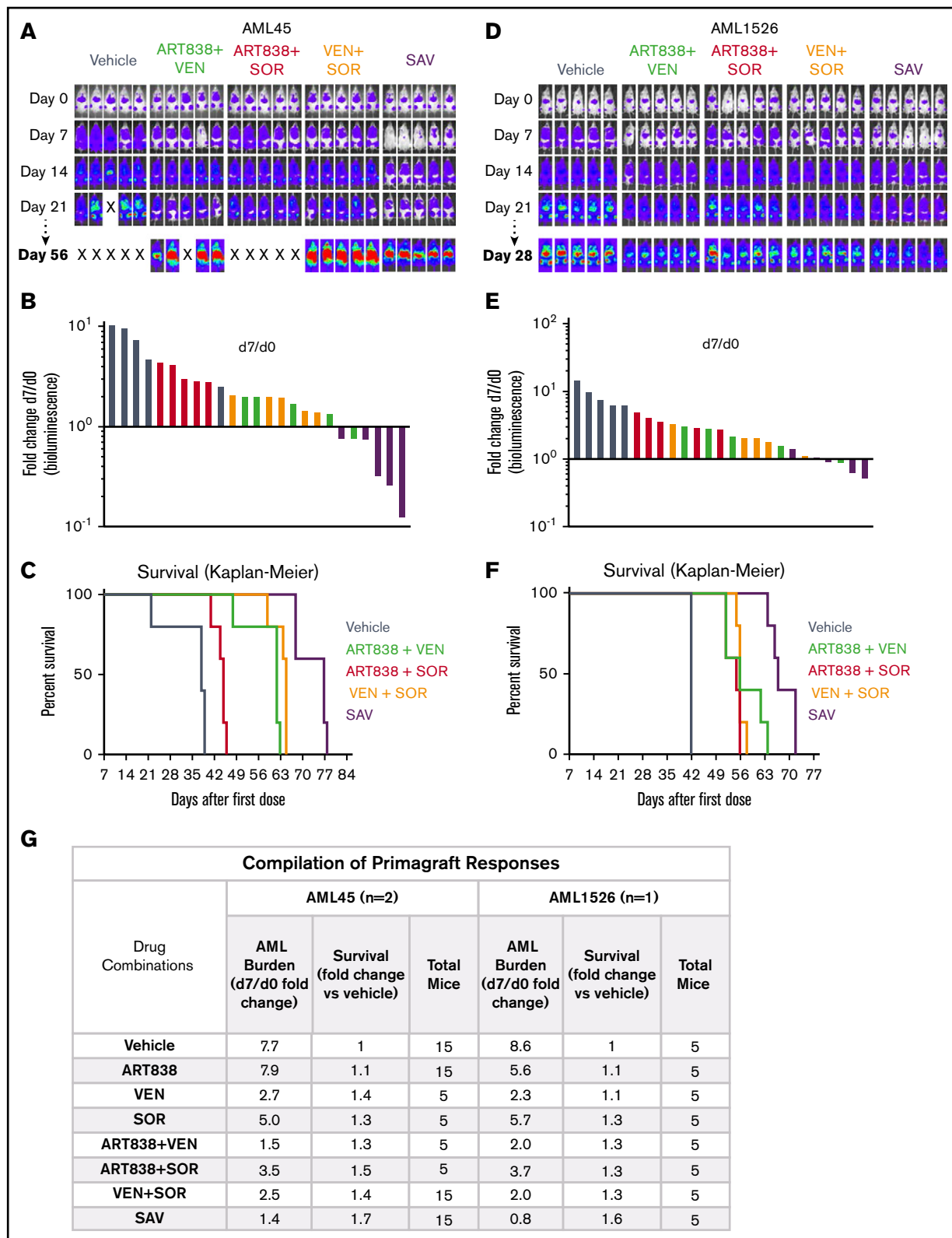
Figure 5. SAV inhibited growth of 2 AML primagrafts. NRG mice bearing luc/YFP-labeled AML45 (A-C) and AML1526 (D-F) primagrafts were performed and data analyzed as in Figure 3. (A,D) BLI of each mouse at each time point in 1 experiment each with AML45 primagraft or AML1526 primagraft model, respectively. (B,E) Waterfall plots depict fold-change in luminescence on day 7 vs day 0 for each mouse, for primagraft experiments using AML45 and AML1526, respectively. (C,F) Kaplan-Meier survival plots for primagraft experiments using AML45 and AML1526, respectively. (C) Comparisons of vehicle vs ART838 plus VEN, vehicle vs ART838 plus SOR, vehicle vs VEN plus SOR, vehicle vs SAV, SAV vs ART838 plus VEN, SAV vs ART838 plus SOR, SAV vs VEN plus SOR all have $P < .005$. (F) Comparisons of vehicle vs ART838 plus VEN,

Similar results were observed in the MV4;11 AML xenograft model (Figure 4E-G; supplemental Figure 16A). Treatment with SAV or each of the 2-drug combinations substantially reduced day 7 AML burdens (Figure 4E-F). VEN plus SOR and SAV extended survival by threefold over vehicle (Figure 4G). All 5 mice from the VEN plus SOR group and 4 of 5 from the SAV group had undetectable AML burdens at experiment termination on day 91 (treatment completed on day 60; supplemental Figure 16A). These interpretations, summarized in Figure 4H, were confirmed by statistical analysis of all experiments in supplemental Figures 15 and 16, (not dependent on censoring of mice that died with low AML burdens). There was a highly significant inverse association between day 7/day 0 fold-change in AML burden and fold-change in survival relative to vehicle for MOLM14 (Spearman rank correlation coefficient, $Rs = -0.98$; $P < .0001$) and MV4;11 AML xenografts ($Rs = -0.97$; $P < .0001$). Because VEN plus SOR was highly effective against both these xenograft models, these models could not definitively ascertain the contribution of ART838 in SAV.

Treatment regimens were tolerated by NRG mice

AML-bearing mice tolerated all treatment regimens without adverse clinical signs or treatment-limiting weight loss ($<20\%$), and there were few unexpected deaths of mice with AML burdens undetectable or lower than on day 0 (censored in Figure 4). Blood cell counts were not significantly reduced in non–AML-bearing mice treated in parallel (supplemental Figure 17).

SAV treatment slowed growth of 2 AML primagraft models

Each of the single drugs and combinations slowed the increase in AML burden over time vs vehicle using the luc/YFP-labeled human AML45 primagraft model,[66] but day 7 AML burden was reduced to below day 0 in only the SAV group and 1 of the ART838 plus VEN mice (Figure 5A-B; supplemental Figure 18A). All mice had AML burdens exceeding day 0 at all subsequent time points (supplemental Figure 18A). The SAV group had the longest survival (Figure 5C; twofold over vehicle). Figure 5G summarizes this and an additional experiment (supplemental Figure 18B) evaluating AML45 primagrafts. SAV was the most active regimen against AML45 primagrafts, and ART838 plus VEN was next best combination.

Similar results were obtained in our luc/YFP-AML1526 primagraft model, with SAV the most effective regimen (survival extended 1.6-fold over vehicle; supplemental Figure 19; Figure 5D-G). VEN plus SOR and ART838 plus VEN had modest effects on AML1526 burden and survival, and ART838 plus SOR was the least active combination.

As with the xenograft models, there was a significant inverse association between the day 7/day 0 fold-change in AML burden and survival for AML45 (Spearman rank correlation coefficient, $Rs = -0.71$; $P = .048$) and AML1526 primagrafts ($Rs = -0.71$; $P = .050$).

Discussion

Artemisinins are cytotoxic to many acute leukemia cell lines,[18-20,23,25] suggesting that the potent ART838 analog, which we found to have favorable stability and pharmacokinetics, might serve as a component of leukemia treatment regimens. From our previous report that 3 tested kinase inhibitors (midostaurin, lestaurtinib, and SOR) each synergized with artemisinins,[18] we chose to combine ART838 with SOR because SOR is a potent inhibitor of the FLT3-ITD mutation common in AML and also inhibits several other kinases (eg, KIT, PDGFR, VEGFR) that may be mutated or overexpressed to drive acute leukemias.[67,68] Moreover, SOR is approved by the US Food and Drug Administration (FDA), has modest toxicity,[69] and is an effective addition to standard clinical AML treatment regimens.[70,71] In this project, our goals were to identify an additional antileukemic drug that might be combined synergistically with SOR and ART838, and then to begin to evaluate this empirically derived 3-drug regimen for efficacy, mechanism, and tolerability, focusing on poor-prognosis AMLs harboring FLT3-ITD and/or MLLr mutations.[72,73]

Our screen of a library of targeted antineoplastics[37-43] revealed that both BCL2 inhibitors in the drug library, ABT737 and VEN, synergized strongly with ART838 (and AS). In vitro culture with ART838 plus VEN robustly reduced growth and enhanced apoptotic cell death of several human acute leukemia cell lines (5 AMLs, 2 ALLs) and primary acute leukemia samples (5 AMLs, 1 ALL), validating the results of the screen. Previous studies indicated that artemisinins induced high cellular levels of reactive oxygen species (ROS), triggered proapoptotic signaling,[18,30,74-76] and altered expression of BCL2 family members in several cancer types.[77-79] Notably, a recent study aimed at identifying drugs that synergize with the dual BCL2/BCLxL inhibitor, NAV, against poor-prognosis B-precursor ALLs harboring the BCR-ABL translocation, found that DHA synergized strongly.[20] Thus, both this and our own validated screen identified that artemisinins and inhibitors of BCL2 family members synergize against at least some acute leukemias, and our results extended this synergy beyond BCR-ABL$^+$ ALLs. Because NAV induced thrombocytopenia in clinical trials,[51,80] we focused on the selective BCL2 inhibitor, VEN. Clinical trials of VEN as a single agent document an encouraging response frequency in AML, but responses were typically only partial and transient.[11] VEN combined with azacytidine or decitabine showed efficacy and low toxicity, which led to FDA approval of VEN-based combination regimens for frail senior patients, poor candidates for standard intensive AraC/anthracycline induction chemotherapy.[81] Finally, SOR and VEN synergize against AML cell lines and patient samples in vitro.[82]

Further understanding of ART838's mechanism(s) of action might explain its empiric synergies with SOR and VEN and suggest additional drugs that might cooperate. All artemisinins contain an endoperoxide pharmacophore(s), which upon activation by iron, induces high levels of intracellular ROS, necessary for artemisinins' antimalarial and antileukemic activities.[30,74-76,83] High-level ROS evokes integrated stress response,[20,84,85] cell-cycle arrest,[18,86] and

---

Figure 5. (continued) vehicle vs ART838 plus SOR, vehicle vs VEN plus SOR, vehicle vs SAV, SAV vs ART838 plus VEN, SAV vs ART838 plus SOR, SAV vs VEN plus SOR all have $P < .005$, by log-rank (Mantel-Cox) test. (G) Aggregated results of 2 AML45 primagraft experiments and 1 AML1526 experiment are summarized. Inverse association between the fold-change (day 7/d 0) in AML burden and fold-change in median survival relative to vehicle for both AML45 and AML1526 were calculated using the Spearman rank correlation coefficient. nd, not done; "X", mouse death.

lysosomal disruption.[87] We assessed several proteins previously shown to regulate MCL1 protein; none were altered by ART838 exposure. Additionally, we inhibited mRNA translation, which did not significantly alter MCL1 protein abundance in the presence of ART838. This experiment takes into account only protein half-life; it does not rule out the possible modulation of MCL1 protein translation via reduced phosphorylated eIF4B.[88] We confirmed and extended the observation that artemisinins induce the integrated stress response, which increases *DDIT3*/CHOP mRNA/protein and reduces MCL1 protein levels in multiple subtypes of acute leukemia cells in vitro and in vivo,[20] suggesting that MCL1 protein and *DDIT3*/CHOP levels may serve as useful biomarkers of the antileukemic action of ART838 and SAV. Indirect reduction of MCL1 by artemisinins might explain their broad antineoplastic activity and their synergy with inhibitors of BCL2 and BCLxL. Furthermore, SOR has been reported to indirectly reduce MCL1 protein stability by increasing its ubiquitination via GSK3β activation,[89] consistent with our finding that SOR reduced the phosphorylated (inactive) form of GSK3β. Because SOR caused only minor elevations of *DDIT3*/CHOP in acute leukemia cells, ART838 and SOR appear to reduce MCL1 protein predominantly by distinct mechanisms; their combined targeting of MCL1 by discrete pathways may explain their antileukemic synergy.

The SAV combination reduced growth and enhanced apoptotic cell death of all tested leukemia cell lines (3 AMLs, 1 ALL) and primary patient samples (5 AMLs, 1 ALL) in vitro, although the extent of drug synergy may have been obscured in these assays by the high efficacy of 1 to 2 of the 3 drugs or by the high spontaneous ex vivo death rates of some of the primary patient AML cases. For these and other reasons, in vivo evaluations may better model clinical trials. For example, despite their in vitro activity as single drugs in this and previous studies, none of these monotherapies substantially reduced AML burdens in our experiments using 4 AML xenograft/primagraft models. Perhaps we would have detected greater in vivo responses had we used an AML progression model in which the xenograft/primagraft-bearing mice were treated before they had large AML burdens; thereby, we and others have documented the single-agent activity of artemisinin analogs.[18,25] In this project, we chose instead to use more challenging in vivo models in an attempt to reveal the potential clinical impact of the drug combinations. In contrast to single drugs, SAV was significantly active against all 4 AML xenograft/primagraft models, causing deep responses in the MOLM14 and MV4;11 AML xenograft models at day 7, which persisted for months during and after treatment completion, without substantial reductions in mouse complete blood counts or body weights. Several mice had undetectable leukemia-based luminescence at the final imaging done in these experiments. Against MOLM14 and MV4;11 AML xenografts, VEN plus SOR was approximately as active as SAV, and much more active than the other 2-drug combinations. The potency of VEN plus SOR may have obscured recognition of the contribution of ART838 in SAV using these 2 xenograft models.

Despite their in vitro sensitivity, the 2 AML primagraft models, both derived from older adults with relapsed, refractory AMLs, were much less sensitive to all tested drug combinations than the MOLM14 and MV4;11 AML xenografts (both derived from young patients harboring FLT3-ITD and MLLr). Notably, SAV was the most active combination against the AML45 primagraft, reducing day 7

AML burdens below day 0 levels, and the ART838 plus VEN combination was the next most effective combination. SAV was also the most active combination against the AML1526 primagraft model, although it only slowed leukemia growth. Thus, these in vivo results in the 2 AML primagraft models confirmed the observed in vitro synergism among the SAV drugs and the contribution of ART838 to the SAV combination.

In the future, newer kinase inhibitors (eg, gilteritinib) might be investigated for combination with ART838 and VEN, especially for cases harboring FLT3 kinase domain mutations (not inhibited by SOR).[90,91] Combination of ART838 and VEN with hypomethylating agents might also be investigated because combinations of VEN with azacytidine or decitabine are clinically active and tolerable. Although cardiotoxicity has been observed in clinical trials of MCL1-competitive inhibitors (eg, NCT03465540),[92] CDK9 inhibitors (eg, voruciclib, alvocidib, or AZD4573) might synergize with SAV to further reduce MCL1 because CDK9 inhibition reduces MCL1 transcription, whereas ART838 and SOR each reduce MCL1 via posttranscriptional mechanisms.[93-95] Finally, AMLs might resist SAV based on high levels of BCLxL,[96] and therefore selective BCLxL inhibitors or dual BCL2/BCLxL inhibitors (eg, NAV) might be evaluated for use in combination with SAV, although their clinical use would require close attention to platelet counts.[97,98]

In summary, our findings, especially the impressive outcomes of SAV in the MLLr⁺FLT3⁺ MOLM14 and MV4;11 AML xenograft models and the cooperativity of the SAV drugs in the AML primagraft models, demonstrate that ART838 and the SAV combination warrant consideration for clinical development for acute leukemias. In parallel, we suggest preclinical evaluation of additional acute leukemia cell line xenografts and primagrafts, especially those containing FLT3-ITD and/or MLLr driver mutations, as well as exploration of the herein-described modifications of the SAV regimen.

Acknowledgments

Authorship

The current affiliation for B.S.M. is Jacobio (US) Pharmaceuticals Inc., Lexington, MA.

The current affiliation for S.M. is Arcellx Inc., Gaithersburg, MD.

The current affiliation for J.M.F. is AstraZeneca, Gaithersburg, MD.

ORCID profiles: B.S.M., 0000-0001-8045-3066; B.T.M., 0000-0002-1912-6362; S.M.B., 0000-0002-7444-7564; A.E., 0000-0003-3769-3210; M.A.R., 0000-0001-5739-6868; T.J.K., 0000-0003-3095-3788; C.I.C., 0000-0002-9555-4895.

Correspondence: Curt I. Civin, University of Maryland School of Medicine, BRB 14-021, 655 W Baltimore St, Baltimore, MD 21201; e-mail: ccivin@som.umaryland.edu.

References

1. Andersson AK, Ma J, Wang J, et al; St. Jude Children's Research Hospital–Washington University Pediatric Cancer Genome Project. The landscape of somatic mutations in infant MLL-rearranged acute lymphoblastic leukemias. *Nat Genet*. 2015;47(4):330-337.

2. Pieters R, Schrappe M, De Lorenzo P, et al. A treatment protocol for infants younger than 1 year with acute lymphoblastic leukaemia (Interfant-99): an observational study and a multicentre randomised trial. *Lancet*. 2007;370(9583):240-250.

3. June CH, O'Connor RS, Kawalekar OU, Ghassemi S, Milone MC. CAR T cell immunotherapy for human cancer. *Science*. 2018;359(6382):1361-1365.

4. Locatelli F, Schrappe M, Bernardo ME, Rutella S. How I treat relapsed childhood acute lymphoblastic leukemia. *Blood*. 2012;120(14):2807-2816.

5. Howlader N, Noone AM, Krapcho M, et al. *SEER Cancer Statistics Review, 1975-2017*. Bethesda, MD: National Cancer Institute; 2020.

6. Siegel RL, Miller KD, Jemal A. Cancer statistics, 2017. *CA Cancer J Clin*. 2017;67(1):7-30.

7. The American Cancer Society. Key Statistics for Acute Myeloid Leukemia (AML). https://www.cancer.org/cancer/acute-myeloid-leukemia/about/key-statistics.html. Accessed 25 June 2020.

8. Papaemmanuil E, Döhner H, Campbell PJ. Genomic classification in acute myeloid leukemia. *N Engl J Med*. 2016;375(9):900-901.

9. Miles LA, Bowman RL, Merlinsky TR, et al. Single-cell mutation analysis of clonal evolution in myeloid malignancies. *Nature*. 2020;587(7834):477-482.

10. Morita K, Wang F, Jahn K, et al. Clonal evolution of acute myeloid leukemia revealed by high-throughput single-cell genomics [published correction appears in *Nat Commun*. 2020;11(1):5996]. *Nat Commun*. 2020;11(1):5327.

11. Konopleva M, Pollyea DA, Potluri J, et al. Efficacy and biological correlates of response in a phase II study of venetoclax monotherapy in patients with acute myelogenous leukemia. *Cancer Discov*. 2016;6(10):1106-1117.

12. Fischer T, Stone RM, Deangelo DJ, et al. Phase IIB trial of oral Midostaurin (PKC412), the FMS-like tyrosine kinase 3 receptor (FLT3) and multi-targeted kinase inhibitor, in patients with acute myeloid leukemia and high-risk myelodysplastic syndrome with either wild-type or mutated FLT3. *J Clin Oncol*. 2010;28(28):4339-4345.

13. Daver N, Schlenk RF, Russell NH, Levis MJ. Targeting FLT3 mutations in AML: review of current knowledge and evidence. *Leukemia*. 2019;33(2):299-312.

14. Stone RM, Mandrekar SJ, Sanford BL, et al. Midostaurin plus chemotherapy for acute myeloid leukemia with a FLT3 mutation. *N Engl J Med*. 2017;377(5):454-464.

15. Wang F, Travins J, DeLaBarre B, et al. Targeted inhibition of mutant IDH2 in leukemia cells induces cellular differentiation. *Science*. 2013;340(6132):622-626.

16. Miller LH, Su X. Artemisinin: discovery from the Chinese herbal garden. *Cell*. 2011;146(6):855-858.

17. Deeken JF, Wang H, Hartley M, et al. A phase I study of intravenous artesunate in patients with advanced solid tumor malignancies. *Cancer Chemother Pharmacol*. 2018;81(3):587-596.

18. Fox JM, Moynihan JR, Mott BT, et al. Artemisinin-derived dimer ART-838 potently inhibited human acute leukemias, persisted in vivo, and synergized with antileukemic drugs. *Oncotarget*. 2016;7(6):7268-7279.

19. Efferth T, Dunstan H, Sauerbrey A, Miyachi H, Chitambar CR. The anti-malarial artesunate is also active against cancer. *Int J Oncol*. 2001;18(4):767-773.

20. Budhraja A, Turnis ME, Churchman ML, et al. Modulation of navitoclax sensitivity by dihydroartemisinin-mediated MCL-1 repression in BCR-ABL+ B-lineage acute lymphoblastic leukemia. *Clin Cancer Res*. 2017;23(24):7558-7568.

21. Jin M, Shen X, Zhao C, et al. In vivo study of effects of artesunate nanoliposomes on human hepatocellular carcinoma xenografts in nude mice. *Drug Deliv*. 2013;20(3-4):127-133.

22. Zhou X, Sun W-J, Wang W-M, et al. Artesunate inhibits the growth of gastric cancer cells through the mechanism of promoting oncosis both in vitro and in vivo. *Anticancer Drugs*. 2013;24(9):920-927.

23. Efferth T, Sauerbrey A, Olbrich A, et al. Molecular modes of action of artesunate in tumor cell lines. *Mol Pharmacol*. 2003;64(2):382-394.

24. Hou J, Wang D, Zhang R, Wang H. Experimental therapy of hepatoma with artemisinin and its derivatives: in vitro and in vivo activity, chemosensitization, and mechanisms of action. *Clin Cancer Res*. 2008;14(17):5519-5530.

25. Drenberg CD, Buaboonnam J, Orwick SJ, et al. Evaluation of artemisinins for the treatment of acute myeloid leukemia. *Cancer Chemother Pharmacol*. 2016;77(6):1231-1243.

26. Dell'Eva R, Pfeffer U, Vené R, et al. Inhibition of angiogenesis in vivo and growth of Kaposi's sarcoma xenograft tumors by the anti-malarial artesunate. *Biochem Pharmacol*. 2004;68(12):2359-2366.

27. Du J-H, Zhang H-D, Ma Z-J, Ji K-M. Artesunate induces oncosis-like cell death in vitro and has antitumor activity against pancreatic cancer xenografts in vivo. *Cancer Chemother Pharmacol*. 2010;65(5):895-902.

28. Du X-X, Li Y-J, Wu C-L, et al. Initiation of apoptosis, cell cycle arrest and autophagy of esophageal cancer cells by dihydroartemisinin. *Biomed Pharmacother*. 2013;67(5):417-424.

29. Ma H, Yao Q, Zhang A-M, et al. The effects of artesunate on the expression of EGFR and ABCG2 in A549 human lung cancer cells and a xenograft model. *Molecules*. 2011;16(12):10556-10569.

30. Efferth T, Giaisi M, Merling A, Krammer PH, Li-Weber M. Artesunate induces ROS-mediated apoptosis in doxorubicin-resistant T leukemia cells. *PLoS One*. 2007;2(8):e693.

31. Efferth T, Davey M, Olbrich A, Rücker G, Gebhart E, Davey R. Activity of drugs from traditional Chinese medicine toward sensitive and MDR1- or MRP1-overexpressing multidrug-resistant human CCRF-CEM leukemia cells. *Blood Cells Mol Dis*. 2002;28(2):160-168.

32. Posner GH, Ploypradith P, Parker MH, et al. Antimalarial, antiproliferative, and antitumor activities of artemisinin-derived, chemically robust, trioxane dimers. *J Med Chem*. 1999;42(21):4275-4280.

33. Posner GH, Ploypradith P, Hapangama W, et al. Trioxane dimers have potent antimalarial, antiproliferative and antitumor activities in vitro. *Bioorg Med Chem*. 1997;5(7):1257-1265.

34. Mott BT, He R, Chen X, et al. Artemisinin-derived dimer phosphate esters as potent anti-cytomegalovirus (anti-CMV) and anti-cancer agents: a structure-activity study. *Bioorg Med Chem*. 2013;21(13):3702-3707.

35. Kim M, Tan YS, Cheng W-C, Kingsbury TJ, Heimfeld S, Civin CI. MIR144 and MIR451 regulate human erythropoiesis via RAB14. *Br J Haematol*. 2015;168(4):583-597.

36. Creed TM, Baldeosingh R, Eberly CL, et al. The PAX-SIX-EYA-DACH network modulates GATA-FOG function in fly hematopoiesis and human erythropoiesis. *Development*. 2020;147(1):dev177022.

37. Richard NP, Pippa R, Cleary MM, et al. Combined targeting of SET and tyrosine kinases provides an effective therapeutic approach in human T-cell acute lymphoblastic leukemia. *Oncotarget*. 2016;7(51):84214-84227.

38. Leonard JT, Raess PW, Dunlap J, Hayes-Lattin B, Tyner JW, Traer E. Functional and genetic screening of acute myeloid leukemia associated with mediastinal germ cell tumor identifies MEK inhibitor as an active clinical agent. *J Hematol Oncol*. 2016;9:31.

39. Siegel MB, Liu SQ, Davare MA, et al. Small molecule inhibitor screen identifies synergistic activity of the bromodomain inhibitor CPI203 and bortezomib in drug resistant myeloma. *Oncotarget*. 2015;6(22):18921-18932.

40. Huang T-C, Cutler J, Bharne S, et al. Integrated analysis of CRLF2 signaling in acute lymphoblastic leukemia identifies Polo-like kinase 1 as a potential therapeutic target. *Leuk Lymphoma*. 2015;56(5):1524-1527.

41. Geng H, Hurtz C, Lenz KB, et al. Self-enforcing feedback activation between BCL6 and pre-B cell receptor signaling defines a distinct subtype of acute lymphoblastic leukemia. *Cancer Cell*. 2015;27(3):409-425.

42. Zhong J, Sharma J, Raju R, et al. TSLP signaling pathway map: a platform for analysis of TSLP-mediated signaling. *Database (Oxford)*. 2014;2014:bau007.

43. Tyner JW, Yang WF, Bankhead A III, et al. Kinase pathway dependence in primary human leukemias determined by rapid inhibitor screening. *Cancer Res*. 2013;73(1):285-296.

44. Bliss CI. The toxicity of poisons applied jointly. *Ann Appl Biol*. 1939;26(3):585-615.

45. Webb JL. *Enzyme and Metabolic Inhibitors*. New York, NY: Academic Press; 1963.

46. Yan H, Zhang B, Li S, Zhao Q. A formal model for analyzing drug combination effects and its application in TNF-alpha-induced NFkappaB pathway. *BMC Syst Biol*. 2010;4:50.

47. Delbridge ARD, Strasser A. The BCL-2 protein family, BH3-mimetics and cancer therapy. *Cell Death Differ*. 2015;22(7):1071-1080.

48. Leverson JD, Phillips DC, Mitten MJ, et al. Exploiting selective BCL-2 family inhibitors to dissect cell survival dependencies and define improved strategies for cancer therapy. *Sci Transl Med*. 2015;7(279):279ra40.

49. Souers AJ, Leverson JD, Boghaert ER, et al. ABT-199, a potent and selective BCL-2 inhibitor, achieves antitumor activity while sparing platelets. *Nat Med*. 2013;19(2):202-208.

50. Zhang H, Nimmer PM, Tahir SK, et al. Bcl-2 family proteins are essential for platelet survival. *Cell Death Differ*. 2007;14(5):943-951.

51. Mason KD, Carpinelli MR, Fletcher JI, et al. Programmed anuclear cell death delimits platelet life span. *Cell*. 2007;128(6):1173-1186.

52. Chou TC, Talalay P. Quantitative analysis of dose-effect relationships: the combined effects of multiple drugs or enzyme inhibitors. *Adv Enzyme Regul*. 1984;22:27-55.

53. Chou TC. Theoretical basis, experimental design, and computerized simulation of synergism and antagonism in drug combination studies. *Pharmacol Rev*. 2006;58(3):621-681.

54. Caserta TM, Smith AN, Gultice AD, Reedy MA, Brown TL. Q-VD-OPh, a broad spectrum caspase inhibitor with potent antiapoptotic properties. *Apoptosis*. 2003;8(4):345-352.

55. Pakos-Zebrucka K, Koryga I, Mnich K, Ljujic M, Samali A, Gorman AM. The integrated stress response. *EMBO Rep*. 2016;17(10):1374-1395.

56. Mandelli F, Vignetti M, Suciu S, et al. Daunorubicin versus mitoxantrone versus idarubicin as induction and consolidation chemotherapy for adults with acute myeloid leukemia: the EORTC and GIMEMA Groups Study AML-10. *J Clin Oncol*. 2009;27(32):5397-5403.

57. Pophali P, Litzow M. What is the best daunorubicin dose and schedule for acute myeloid leukemia induction? *Curr Treat Options Oncol*. 2017;18(1):3.

58. Kotschy A, Szlavik Z, Murray J, et al. The MCL1 inhibitor S63845 is tolerable and effective in diverse cancer models. *Nature*. 2016;538(7626):477-482.

59. He R, Forman M, Mott BT, Venkatadri R, Posner GH, Arav-Boger R. Unique and highly selective anticytomegalovirus activities of artemisinin-derived dimer diphenyl phosphate stem from combination of dimer unit and a diphenyl phosphate moiety. *Antimicrob Agents Chemother*. 2013;57(9):4208-4214.

60. Alagbala AA, McRiner AJ, Borstnik K, et al. Biological mechanisms of action of novel C-10 non-acetal trioxane dimers in prostate cancer cell lines. *J Med Chem*. 2006;49(26):7836-7842.

61. Kapadia B, Nanaji NM, Bhalla K, et al. Fatty acid synthase induced S6Kinase facilitates USP11-eIF4B complex formation for sustained oncogenic translation in DLBCL. *Nat Commun*. 2018;9(1):829.

62. Gasca J, Flores ML, Giráldez S, et al. Loss of FBXW7 and accumulation of MCL1 and PLK1 promote paclitaxel resistance in breast cancer. *Oncotarget*. 2016;7(33):52751-52765.

63. Zhang S, Zhang M, Jing Y, et al. Deubiquitinase USP13 dictates MCL1 stability and sensitivity to BH3 mimetic inhibitors. *Nat Commun*. 2018;9(1):215.

64. Pan R, Ruvolo V, Mu H, et al. Synthetic lethality of combined Bcl-2 inhibition and p53 activation in AML: mechanisms and superior antileukemic efficacy. *Cancer Cell*. 2017;32(6):748-760.e6.

65. Wang R, Li Y, Gong P, Gabrilove J, Waxman S, Jing Y. Arsenic trioxide and sorafenib induce synthetic lethality of FLT3-ITD acute myeloid leukemia cells. *Mol Cancer Ther*. 2018;17(9):1871-1880.

66. Grimwade D, Hills RK, Moorman AV, et al; National Cancer Research Institute Adult Leukaemia Working Group. Refinement of cytogenetic classification in acute myeloid leukemia: determination of prognostic significance of rare recurring chromosomal abnormalities among 5876 younger adult patients treated in the United Kingdom Medical Research Council trials. *Blood*. 2010;116(3):354-365.

67. Zhang W, Konopleva M, Shi YX, et al. Mutant FLT3: a direct target of sorafenib in acute myelogenous leukemia. *J Natl Cancer Inst*. 2008;100(3):184-198.

68. Lierman E, Lahortiga I, Van Miegroet H, Mentens N, Marynen P, Cools J. The ability of sorafenib to inhibit oncogenic PDGFRbeta and FLT3 mutants and overcome resistance to other small molecule inhibitors. *Haematologica*. 2007;92(1):27-34.

69. Uy GL, Mandrekar SJ, Laumann K, et al. A phase 2 study incorporating sorafenib into the chemotherapy for older adults with FLT3-mutated acute myeloid leukemia: CALGB 11001. *Blood Adv*. 2017;1(5):331-340.

70. Pratz KW, Cho E, Levis MJ, et al. A pharmacodynamic study of sorafenib in patients with relapsed and refractory acute leukemias. *Leukemia*. 2010;24(8):1437-1444.

71. Borthakur G, Kantarjian H, Ravandi F, et al. Phase I study of sorafenib in patients with refractory or relapsed acute leukemias. *Haematologica*. 2011;96(1):62-68.

72. Zimmerman EI, Turner DC, Buaboonnam J, et al. Crenolanib is active against models of drug-resistant FLT3-ITD-positive acute myeloid leukemia. *Blood*. 2013;122(22):3607-3615.

73. Bayat Mokhtari R, Homayouni TS, Baluch N, et al. Combination therapy in combating cancer. *Oncotarget*. 2017;8(23):38022-38043.

74. Hamacher-Brady A, Stein HA, Turschner S, et al. Artesunate activates mitochondrial apoptosis in breast cancer cells via iron-catalyzed lysosomal reactive oxygen species production. *J Biol Chem*. 2011;286(8):6587-6601.

75. Mercer AE, Copple IM, Maggs JL, O'Neill PM, Park BK. The role of heme and the mitochondrion in the chemical and molecular mechanisms of mammalian cell death induced by the artemisinin antimalarials. *J Biol Chem*. 2011;286(2):987-996.

76. Stockwin LH, Han B, Yu SX, et al. Artemisinin dimer anticancer activity correlates with heme-catalyzed reactive oxygen species generation and endoplasmic reticulum stress induction [published correction appears in *Int J Cancer*. 2010;127(11):E1]. *Int J Cancer*. 2009;125(6):1266-1275.

77. Hu CJ, Zhou L, Cai Y. Dihydroartemisinin induces apoptosis of cervical cancer cells via upregulation of RKIP and downregulation of bcl-2. *Cancer Biol Ther*. 2014;15(3):279-288.

78. Kumar B, Kalvala A, Chu S, et al. Antileukemic activity and cellular effects of the antimalarial agent artesunate in acute myeloid leukemia. *Leuk Res*. 2017; 59(suppl C):124-135.

79. Morrissey C, Gallis B, Solazzi JW, et al. Effect of artemisinin derivatives on apoptosis and cell cycle in prostate cancer cells. *Anticancer Drugs*. 2010; 21(4):423-432.

80. Roberts AW, Seymour JF, Brown JR, et al. Substantial susceptibility of chronic lymphocytic leukemia to BCL2 inhibition: results of a phase I study of navitoclax in patients with relapsed or refractory disease. *J Clin Oncol*. 2012;30(5):488-496.

81. US Food and Drug Administration. FDA Approves Venetoclax in Combination for AML in Adults. https://www.fda.gov/drugs/fda-approves-venetoclax-combination-aml-adults. Accessed 28 April 2020.

82. Kurtz SE, Eide CA, Kaempf A, et al. Molecularly targeted drug combinations demonstrate selective effectiveness for myeloid- and lymphoid-derived hematologic malignancies. *Proc Natl Acad Sci USA*. 2017;114(36):E7554-E7563.

83. D'Angelo JG, Bordón C, Posner GH, Yolken R, Jones-Brando L. Artemisinin derivatives inhibit Toxoplasma gondii in vitro at multiple steps in the lytic cycle. *J Antimicrob Chemother*. 2009;63(1):146-150.

84. Bridgford JL, Xie SC, Cobbold SA, et al. Artemisinin kills malaria parasites by damaging proteins and inhibiting the proteasome. *Nat Commun*. 2018;9(1): 3801.

85. Chen Y, Mi Y, Zhang X, et al. Dihydroartemisinin-induced unfolded protein response feedback attenuates ferroptosis via PERK/ATF4/HSPA5 pathway in glioma cells. *J Exp Clin Cancer Res*. 2019;38(1):402.

86. Finaurini S, Basilico N, Corbett Y, et al. Dihydroartemisinin inhibits the human erythroid cell differentiation by altering the cell cycle. *Toxicology*. 2012; 300(1-2):57-66.

87. Sukhai MA, Prabha S, Hurren R, et al. Lysosomal disruption preferentially targets acute myeloid leukemia cells and progenitors. *J Clin Invest*. 2013; 123(1):315-328.

88. Wang Y, Begley M, Li Q, et al. Mitotic MELK-eIF4B signaling controls protein synthesis and tumor cell survival. *Proc Natl Acad Sci USA*. 2016;113(35): 9810-9815.

89. Wang R, Xia L, Gabrilove J, Waxman S, Jing Y. Sorafenib inhibition of Mcl-1 accelerates ATRA-induced apoptosis in differentiation-responsive AML cells. *Clin Cancer Res*. 2016;22(5):1211-1221.

90. Nguyen B, Williams AB, Young DJ, et al. FLT3 activating mutations display differential sensitivity to multiple tyrosine kinase inhibitors. *Oncotarget*. 2017; 8(7):10931-10944.

91. Tarver TC, Hill JE, Rahmat L, et al. Gilteritinib is a clinically active FLT3 inhibitor with broad activity against FLT3 kinase domain mutations. *Blood Adv*. 2020;4(3):514-524.

92. Amgen Highlights New Data From KYPROLIS (carfilzomib) And Oncology Pipeline At IMW 2019. Thousand Oaks, CA: Amgen, Inc; 2019.

93. Luedtke DA, Su Y, Ma J, et al. Inhibition of CDK9 by voruciclib synergistically enhances cell death induced by the Bcl-2 selective inhibitor venetoclax in preclinical models of acute myeloid leukemia. *Signal Transduct Target Ther*. 2020;5(1):17.

94. Zeidner JF, Karp JE. Clinical activity of alvocidib (flavopiridol) in acute myeloid leukemia. *Leuk Res*. 2015;39(12):1312-1318.

95. Cidado J, Boiko S, Proia T, et al. AZD4573 is a highly selective CDK9 inhibitor that suppresses MCL-1 and induces apoptosis in hematologic cancer cells. *Clin Cancer Res*. 2020;26(4):922-934.

96. Caenepeel S, Brown SP, Belmontes B, et al. AMG 176, a selective MCL1 inhibitor, is effective in hematologic cancer models alone and in combination with established therapies. *Cancer Discov*. 2018;8(12):1582-1597.

97. Khaw SL, Suryani S, Evans K, et al. Venetoclax responses of pediatric ALL xenografts reveal sensitivity of MLL-rearranged leukemia. *Blood*. 2016; 128(10):1382-1395.

98. Pan R, Ruvolo VR, Wei J, et al. Inhibition of Mcl-1 with the pan-Bcl-2 family inhibitor (-)BI97D6 overcomes ABT-737 resistance in acute myeloid leukemia. *Blood*. 2015;126(3):363-372.

99. Tanavde VM, Malehorn MT, Lumkul R, et al. Human stem-progenitor cells from neonatal cord blood have greater hematopoietic expansion capacity than those from mobilized adult blood. *Exp Hematol*. 2002;30(7):816-823.